

Synthesis, Characterizations, and Physical Properties of Carbon Nanotubes Coated by Conducting Polypyrrole

JUNHUA FAN,¹ MEIXIANG WAN,¹ DAOBEN ZHU,¹ BAOHE CHANG,² ZHENWEI PAN,² SISHEN XIE²

¹ Institute of Chemistry, The Chinese Academy of Sciences, Beijing 100080, People's Republic of China

² Institute of Physics, The Chinese Academy of Sciences, Beijing 100080, People's Republic of China

Received 12 November 1998; accepted 20 March 1999

ABSTRACT: A new type of carbon nanotube (CNT) (diameter of <100 nm) coated by conducting polypyrrole (PPY) was synthesized by *in situ* polymerization on CNTs. The structure of the resulting complex nanotubes (CNT-PPY) was characterized by elemental analysis, X-ray photoelectron spectroscopy, Raman spectra, and X-ray diffraction. These indicated no significant chemical interaction between PPY and the CNT. The electrical, magnetic, and thermal properties of the complex nanotubes were measured and showed the physical properties of the CNTs were modified by conducting PPY. © 1999 John Wiley & Sons, Inc. *J Appl Polym Sci* 74: 2605–2610, 1999

Key words: carbon nanotubes; conducting polypyrrole; *in situ* polymerization

INTRODUCTION

Since the discovery¹ and bulk synthesis² of carbon nanotubes (CNTs), great interest has been stimulated for their potential applications in nanoscale devices and materials,^{3,4} field emission,⁵ and scanning probe microscopy.⁶ Various approaches have been developed for opening up^{7–9} the CNT ends and encapsulating material^{7,9,10} to form a nanocomposite, which might be used in catalyst, separation, and storage technology and in the development of materials with new magnetic and electrical properties.¹¹

On the other hand, conductive polymer microtubes have attracted much attention because of their applications in drug delivery systems,^{12,13} microwave components after coating with metal, and electronic and electrooptical devices.¹⁴ In

general, the “template synthesis” method, which involves using pores in a microporous membrane as a template for microtube formation, is an effective method to synthesize tubular conducting polymers. The template synthesized method proposed by Georger et al.¹⁵ was successfully applied in the synthesis of polyacetylene,¹⁶ poly(3-methylthiophene),¹⁷ polypyrrole (PPY)¹⁸ and polyaniline¹⁹ tubes. Recently, a simple method of *in situ* doping polymerization in the presence of β -naphthalene sulfonic acid as the dopant was proposed by Wan et al.²⁰ to synthesize tubular polyaniline²¹ and PPY.²² Compared to the template synthesis method, *in situ* doping polymerization is much simpler without the microporous membrane as the template or even a “molecular anchor” to bind the polymer to the wall of the microporous membrane. Moreover, among the conducting polymers, conducting PPY as a typical conducting polymer has important commercial application because of its high conductivity, easy synthesis, and long-term stability in air. Therefore, we expected it to be very interesting to modify CNTs by coating the conducting PPY to form complex CNTs.

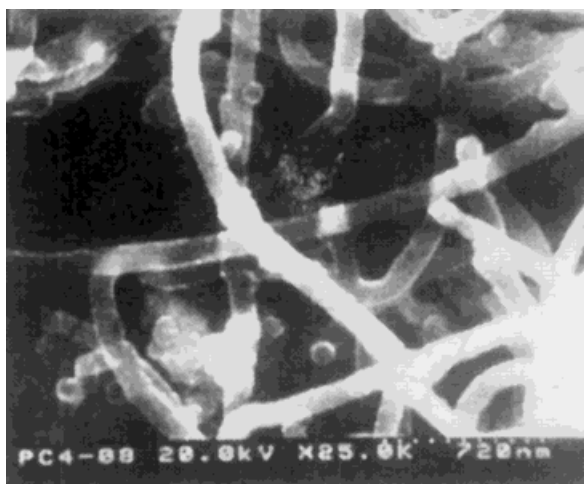
Correspondence to: M. Wan (wanmx@infoc3.icas.ac.cn).

Contract grant sponsors: Chinese Academy of Sciences; Director Foundation of the Institute of Chemistry, Chinese Academy of Sciences

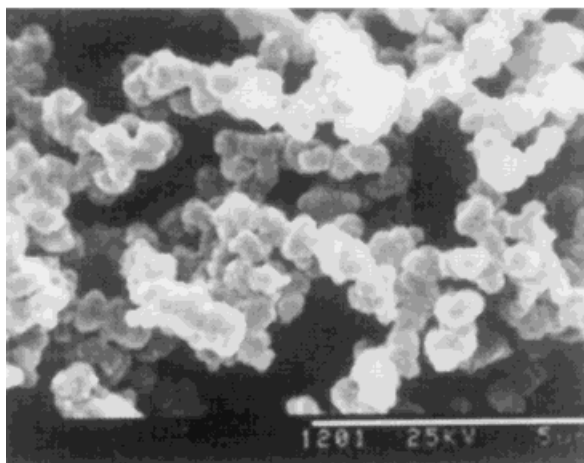
Journal of Applied Polymer Science, Vol. 74, 2605–2610 (1999)

© 1999 John Wiley & Sons, Inc.

CCC 0021-8995/99/112605-06



(a)



(b)

Figure 1 SEM images of (a) CNT-PPY and (b) PPY nanotubes.

In this article, a new type of CNT was coated by conducting PPY and was synthesized by *in situ* polymerization of pyrrole on CNTs. The structure of the resulting complex nanotubes (CNT-PPY) was characterized and their electrical, magnetic, and thermal properties were discussed.

EXPERIMENTAL

Pyrrole monomer was distilled under reduced pressure. Ammonium persulfate (oxidant), hydrochloric acid, and other organic solvents were used as received without further treatment. The CNTs were synthesized using thermal deposition of hydrocarbons.⁴

CNT-PPY nanotubes were synthesized by *in situ* polymerization of pyrrole on CNTs. A typical synthesis routine is as follows: 150 mL of 0.1M HCl solution containing CNTs (0.2 g) was sonicated at room temperature for about 0.5 h to disperse the CNTs. Pyrrole monomer (0.67 g) in 100 mL of HCl (0.1M) solution was added to the above CNT suspension solution. A 50 mL HCl (0.1M) solution containing $(\text{NH}_4)_2\text{S}_2\text{O}_8$ (0.82 g) was slowly added dropwise into the suspension solution with constant sonication at a reaction temperature of 0–5°C. The reaction mixture was sonicated for an additional 4 h at 0–5°C, after which the CNT-PPY powder formed was filtered and rinsed with distilled water and methanol until the filtrate was colorless. The obtained black powder was dried under a vacuum at room temperature for 24 h.

We found that a stable suspension of well-separated CNTs is a key factor to preparing uniform CNT-PPY nanotubes. Therefore, the reaction was carried out with constant sonication throughout the whole polymerization process and a very dilute reaction solution was used. In this way uniform images of the CNT-PPY nanotubes were obtained by scanning electron microscopy (SEM) as shown in Figure 1(a). The tubular morphology of CNT-PPY with a diameter of 0.1 μm was confirmed by a high-resolution transmission electron microscope (TEM) as shown in Figure 2. From Figure 1(b) one can see that the pure PPY synthesized without CNTs shows a typical granular morphology, which is consistent with previous observations.²³ Compared to the pure CNTs, the CNT-PPY nanotubes are very thick (80–100 nm diameter) and their external surface is not smooth.

The elemental analysis was performed by the Analytical Laboratory in our institute (Heraeus,

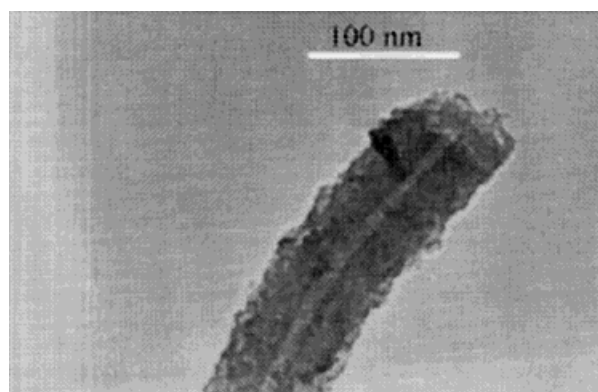


Figure 2 TEM images of CNT-PPY nanotubes.

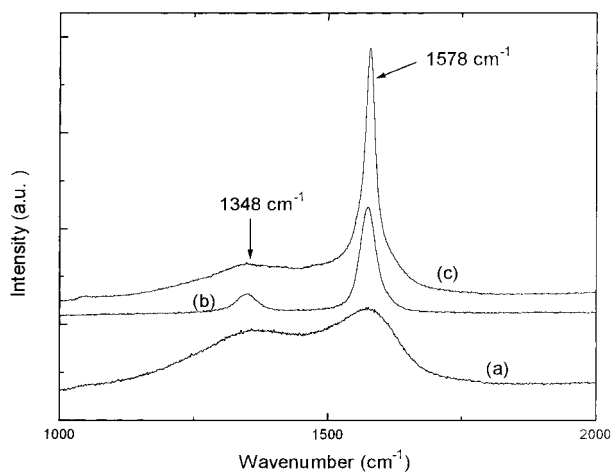


Figure 3 Raman spectra of (a) PPY, (b) CNT, and (c) CNT-PPY nanotubes.

CHN-Rapid). SEM images were examined by an S-4200. The high-resolution TEM imaging was performed with a JEM-200CX. The Raman spectra were carried out on a Renishaw 1000 spectrometer. The X-ray diffraction was measured by an MP18HF (Mac Science, Japan). The room-temperature conductivities of pressed pellets were measured by the conventional four-probe method using an Advantest R6142 programmable DC voltage/current generator and a Keithley 196 system DMM. The temperature dependence of the conductivity was measured at temperatures between 50 and 300 K by the four-probe method. A Keithley 2002 multimeter was used to measure the voltage. The temperature was controlled by a Lakeshore DRC-91CA temperature controller. Electron spin resonance (ESR) measurements were carried out on a Bruker ER-200D. Thermal gravimetric analyses (TGA) were conducted on a Perkin-Elmer TGA-7 under a nitrogen atmosphere with a heating rate of 10°C/min. The magnetization with the applied magnetic field at 1.5 K was measured using an extracting sample magnetometer (Neel Laboratory CF-1).

RESULTS AND DISCUSSION

Structural Characterization

The structure of the resulting CNT-PPY nanotubes was characterized by elemental analysis, X-ray photoelectron spectroscopy (XPS), and Raman spectra, as well as X-Ray diffraction. Elemental analysis data show that the composition

of the PPY and CNT in the CNT-PPY nanotubes is about 1 : 1 (wt %): C 56.49, H 3.28, and N 15.88 for PPY; C 99.42 for CNT; and C 78.36, H 1.56, and N 7.20 for CNT-PPY.

Typical Raman spectra for PPY, CNT, and CNT-PPY were measured by using an Ar laser at 514.5 nm as the laser source (Fig. 3). The typical peak of pure CNTs at 1581 cm^{-1} comes from the E_{2g} mode.²⁴ It has also been theoretically deduced that a single-cylinder nanotube should show an E_{2g} mode at 1601 cm^{-1} .²⁵ The band at 1350 cm^{-1} appears only in slightly disordered graphite.²⁶ On the other hand, the Raman spectrum of pure PPY shows a broad band at 1300–1600 cm^{-1} in the C=C stretching vibration range, which is similar to the report by Cheung et al.²⁷ However, no new bands were observed from the Raman spectrum of CNT-PPY nanotubes except the characteristic peaks of CNT and PPY. This indicates that there are no new chemical bands formed in CNT-PPY nanotubes between the CNT and PPY.

The X-ray scattering pattern for CNT, PPY, and CNT-PPY are shown in Figure 4. The broad band for PPY centered at $2\theta = 25^\circ$ is assigned to pyrrole interchain spacings, which is in accordance with a previous report.²⁸ The pure CNT has characteristic peaks at 3.42, 2.13, and 1.70 Å in good agreement with a previous report.²⁹ For CNT-PPY nanotubes the X-ray diffraction shows the characteristic broad peak of PPY and the strong peaks of CNT. However, no new peaks appear.

The XPS analyses of PPY, CNT, and CNT-PPY nanotubes are given in Table I. The N1s spectrum of PPY shows two peaks at a binding energy of

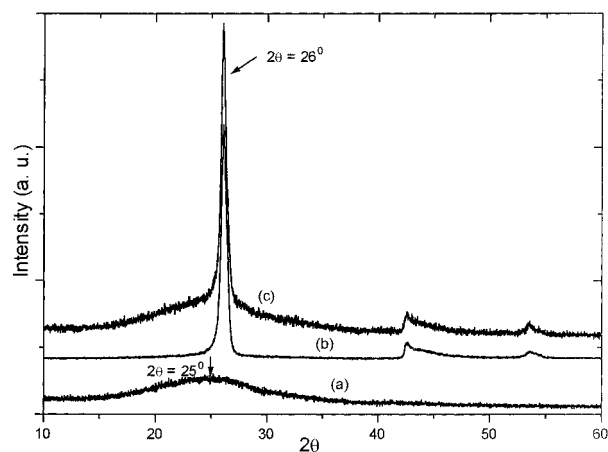


Figure 4 X-ray diffraction of (a) PPY, (b) CNT, and (c) CNT-PPY nanotubes.

Table I XPS Analysis for CNT, PPY, and CNT-PPY Nanotubes

Sample	PPY	CNT	CNT-PPY
C1s (eV)	284.53	284.64	284.54
	286.91	287.00	287.05
	289.43	291.03	289.63
N1s (eV)	399.50		399.52
	402.05		402.06

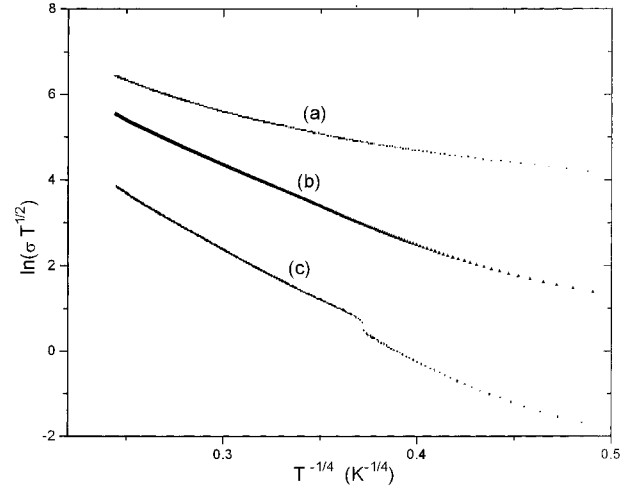
about 399.5 eV, which is characteristic of the pyrrolium nitrogens ($-\text{NH}$ structure), and a high binding energy tail (center at 402.05 eV) attributable to the positively charged nitrogen ($-\text{N}^+\text{H}-$ structure).³⁰ The N1s spectrum of CNT-PPY is at the same position, meaning that the chemical environment of the N element in pure PPY and CNT-PPY is almost identical. Similarly, the C1s core-level spectra for pure PPY and CNT-PPY are also in good agreement. According to the discussions above, this suggests that no chemical reaction between CNT and PPY takes place and the CNTs just function as a template for the polymerization of conducting PPY.

Electrical Properties

The room-temperature conductivity of PPY synthesized by the chemical method is about 3.0 S/cm lower than that by the electrochemical method (σ_{RT} in the range of 20–100 S/cm)³¹ but is higher than that by the chemical method using FeCl_3 as the oxidant ($\sigma_{\text{RT}} = 0.07$ S/cm).¹¹ The room-temperature conductivity of an unaligned CNT pellet by the four-probe method is 40 S/cm, which is much lower than that of a single CNT³² due to the tube–tube contact resistance. The conductivity of CNT-PPY nanotubes at room temperature is about 16 S/cm, which is in between CNT and PPY as given in Table II.

Table II Electrical Properties of CNT, PPY, and CNT-PPY Nanotubes

Sample	σ_{RT} (S/cm)	Temp. Dependence of Conductivity	Deviation Temp. (K)	T_0 (K)
PPY	3	3-D-VRH	52	3.9×10^5
CNT	50	3-D-VRH	110	2.5×10^4
CNT-PPY	16	3-D-VRH	27	1.6×10^5

**Figure 5** The temperature dependence of conductivity for (a) CNT, (b) CNT-PPY nanotubes, and (c) PPY.

As we know, polarons and bipolarons as charge carriers can be distinguished by ESR measurements. We found that the purified CNT is almost ESR silent at room temperature, which is consistent with the previous report.³³ However, the pure PPY shows the ESR signal with a g value of 2.003, indicating the presence of a polaron in PPY.³⁴ The results from the combination of the ESR measurement and UV-visible spectra of PPY indicate that the polaron and bipolaron both serve as charge carriers in PPY. A strong ESR signal with a g value of 2.003 in the CNT-PPY nanotubes was observed, which means the type of charge carriers in the CNT-PPY nanotubes is dominated by PPY. Note that a slight difference in the line width (ΔH) of the ESR signal between pure PPY and CNT-PPY nanotubes was observed. For instance, the line width of 2.7 G for pure PPY and 5.0 G for CNT-PPY nanotubes was obtained. This difference may be due to the difference in spin–spin and spin–lattice relaxation time between them.

The conductivity of PPY, CNT, and CNT-PPY increases with an increase of temperature, which is a typical characteristic of semiconductor behavior. The 3-dimensional (3-D) variable range hopping (VRH) model provides the best fit to the data as shown in Figure 5.

According to the 3-D-VRH model,³² the following equation can be obtained:

$$\sigma_{\text{dc}} = \sigma_0 \exp[-(T_0/T)^{1/4}], \quad (1)$$

where $T_0 = 8\alpha/(zN(E_F)k_B)$, α^{-1} is the localization length, $N(E_F)$ is the density of states at the

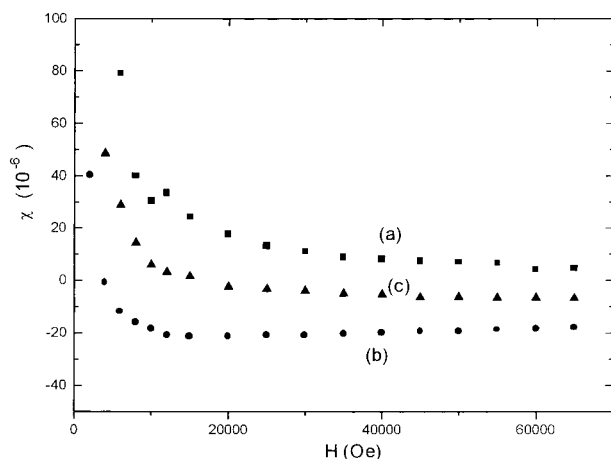


Figure 6 Magnetic field dependence of the magnetic susceptibility of (a) CNT, (b) PPY, and (c) CNT-PPY nanotubes.

Fermi level, k_B is the Boltzmann constant, and z is the number of nearest neighbor chains. Plotting $\ln \sigma_{dc}$ versus $T^{-1/4}$, the T_0 can be obtained from the slope. The T_0 value of the CNTs is calculated to be 2.5×10^4 K, which is much lower than that of PPY (3.9×10^5 K), corresponding to the high room-temperature conductivity of CNTs. The fact that the T_0 value of the CNT-PPY nanotube (1.6×10^5 K) is lower than that of PPY indicates that the electrical properties of PPY are enhanced after coating on CNTs. Moreover, Figure 5 shows that the data do not fit the 3-D-VRH model at a lower temperature. The deviation temperature from the VRH model is different for CNT, PPY, and CNT-PPY nanotubes (Table II).

Magnetic Properties

The magnetizations of CNT, PPY, and CNT-PPY nanotubes were measured at varied magnetic fields from 0 to 6.5×10^4 Oe at 1.5 K. The dependence of the static magnetic susceptibility (χ) with the applied magnetic field is shown in Figure 6. We found that the magnetic susceptibility of the three samples decreases with an increasing magnetic field in the low magnetic field (0–15000 Oe). However, at a high magnetic field ($H > 15,000$ Oe) the magnetic susceptibility is independent of the magnetic field. The positive magnetic susceptibility of PPY is calculated to be 5×10^{-6} emu/g, consistent with a previous report.³⁴ The negative magnetic susceptibility of CNT is calculated to be 18×10^{-6} emu/g, similar to a previous report.³⁵

We found very interesting to find that the magnetic susceptibility of CNT-PPY nanotubes is al-

most equal to that of the sum of the CNTs and PPY. From the elemental analysis (Table II) we noted that the content of CNT and PPY in the CNT-PPY nanotubes is about 1 : 1 (w/w). Therefore, the magnetic measurements and elemental analysis are in good agreement.

Thermal Stability

TGA is a useful method for testing the thermal stability of polymers. Figure 7 shows a comparison of the mass losses of CNT, PPY, and CNT-PPY nanotubes upon heating in a nitrogen atmosphere. CNTs are very stable and no decomposition takes place in the range of 0–800°C. PPY displays a steady decrease in mass near 10% at temperatures between 100 and 288°C. However, a rapid change in mass occurs in the range of 300–800°C, and only a 10% mass is reserved. Below 100°C the decomposition is due to a small part of water or dedoping in the sample. CNT-PPY nanotubes exhibit good stability under nitrogen, showing a slight plateau (about 3% mass loss) from 100 until 300°C, after which the degradation rate increases. Up to 800°C the decomposition mass is about 54%. Because the trend of the degradation curve of CNT-PPY nanotubes is similar to that of PPY, the degradation of the CNT-PPY nanotubes is mainly controlled by PPY.

CONCLUSIONS

Complex nanotubes of CNTs coated with PPY were synthesized by *in situ* polymerization of pyr-

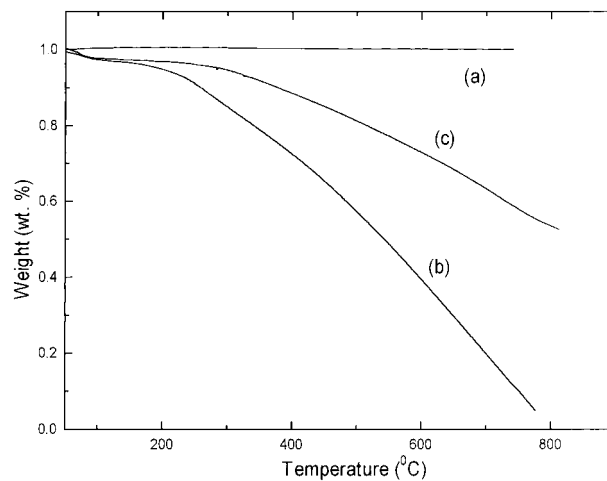


Figure 7 Thermal stability of (a) CNT, (b) PPY, and (c) CNT-PPY nanotubes under a nitrogen atmosphere.

role monomer on CNTs. The structural characterizations indicated that no chemical reaction between the CNTs and PPY takes place; the CNTs only function as a template for polymerization of PPY. The electrical, magnetic, and thermal properties of the CNTs were modified by PPY.

REFERENCES

- Iijima, S. *Nature* 1991, 354, 56.
- Ebbesen, T. W.; Ajayan, P. M. *Nature* 1992, 358, 220.
- Ebbesen, T. W. *Phys Today* 1996, June, 26.
- Treay, M. M. J.; Ebbesen, T. W.; Gibson, J. M. *Nature* 1996, 381, 678.
- de Heer, W. A.; Châtelain, A.; Ugarte, D. *Science* 1995, 270, 1179.
- Dai, H.; Hafner, J. H.; Rinzler, A. G.; Colbert, D. T.; Smalley, R. E. *Nature* 1996, 384, 147.
- Ruoff, R. S.; Lorents, D. C.; Chan, B.; Malhotra, R.; Subramoney, S. *Science* 1993, 259, 346.
- Tomita, M.; Saito, Y.; Hayashi, T. *Jpn J Appl Phys* 1993, 32, L280.
- Seraphin, S.; Zhou, D.; Jiao, J.; Withers, J. C.; Loufty, R. *Nature* 1993, 362, 503.
- Saito, Y.; Yoshikawa, T.; Okuda, M.; Ohkohchi, M.; Ando, Y.; Kasuya, A.; Nishina, Y. *Chem Phys Lett* 1993, 209, 72.
- Tsang, S. C.; Chen, Y. K.; Harris, P. J. F.; Green, M. L. H. *Nature* 1994, 372, 159.
- Rudolph, A. S.; Calvert, J. M.; Schoen, P. E. In *Biotechnological Applications of Lipid Microstructures*; Caber, B. P.; Schnur, J. M.; Chapman, D., Eds.; Plenum: New York, 1988.
- Pool, R. *Science* 1990, 247, 448.
- Tabony, J.; Tob, D. *Nature* 1990, 346, 448.
- Georger, J. H.; Singh, A.; Price, R. P.; Schnur, J. M.; Yager, P.; Schoen, P. E. *J Am Chem Soc* 1987, 109, 6169.
- Liang, W.; Martin, C. R. *J Am Chem Soc* 1991, 112, 9666.
- Cai, Z.; Martin, C. R. *J Am Chem Soc* 1989, 111, 4138.
- Cai, Z.; Lei, J.; Liang, W.; Menon, V.; Martin, C. R. *Chem Mater* 1990, 3, 960.
- Martin, C. R.; Parthasarathy, R.; Menon, V. *Synth Metals* 1993, 55, 1165.
- Wan, M. X.; Shen, Y. Q.; Huang, J. *Chin. Pat. Applic.* 98,109,916.5 (1998).
- Huang, J.; Wan, M. X. *J Polym Sci* to appear.
- Shen, Y. Q.; Wan, M. X. *J Polym Sci* to appear.
- Shen, Y. Q.; Wan, M. X. *J Appl Polym Sci* 1998, 68, 1277.
- Hlura, H.; Ebbesen, T. W.; Tanigaki, T.; Takahashi, H. *Chem Phys Lett* 1993, 202, 509.
- Jishi, R. A.; Venkataran, L.; Dresselhaus, M. S.; Dresselhaus, G. *Chem Phys Lett* 1993, 209, 77.
- de Heer, W. A.; Bacsá, W. S.; Chatelain, A.; Gerfin, T.; Humphrey-Baker, R.; Forro, L.; Ugarte, D. *Science* 1995, 268, 845.
- Bates, N.; Cross, M.; Lines, R.; Walton, D. *J Chem Soc Chem Commun* 1985, 871.
- Wynne, J.; Street, G. B. *Macromolecules* 1985, 18, 2361.
- Zhou, O.; Fleminy, R. M.; Murphy, D. W. *Science* 1994, 263, 744.
- Tan, K. L.; Tan, B. T. G.; Kang, E. T.; Neoh, K. G. *J Mater Sci* 1992, 27, 4056.
- Ogasawara, M.; Funahashi, K.; Demura, T.; Hagiwara, T.; Iwata, K. *Synth Metals* 1986, 14, 61.
- Shklovskii, B. I.; Efros, A. L. *Electronic Properties of Doped Semiconductors*; Springer-Verlag: Berlin, 1985.
- Tanaka, K.; Sato, T.; Yamabe, T.; Okahara, K.; Uchida, K.; Yumura, M.; Niino, H.; Ohshima, S.; Kuriki, Y.; Yase, K.; Ikazaki, F. *Chem Phys Lett* 1994, 223, 65.
- Mizoguchi, K.; Kachi, N.; Sakamoto, H.; Kume, K.; Yoshioka, K.; Masubuchi, S.; Kazama, S. *Synth Metals* 1997, 84, 695.
- Wang, X. K.; Chang, R. P. H.; Patashinski, A.; Ketterson, J. B. *J Mater Res* 1994, 9, 1578.